Limitations of Conventional Internal Dosimetry at the Cellular Level

G. Mike Makrigiorgos, S. James Adelstein, and Amin I. Kassis

Department of Radiology, Harvard Medical School, Shields Warren Radiation Laboratory, Boston, Massachusetts

A theoretic examination of the validity at the cellular level of assumptions used in classic internal dosimetry has been undertaken. An alternate dosimetric model accounting for the consequences of selective uptake of a radiolabeled compound by specific cells in a multicellular cluster of hexagonal geometry has been developed. At the cellular level, derived dose estimates for electrons have been compared to dose estimates obtained employing the assumptions of conventional internal dosimetry. The study has been performed for all electron energies and then applied specifically to electrons emitted by ^{99m}Tc, ^{201}Tl, ^{111}In, and ^{123}I. The dosimetric consequences of altering (a) the intracellular-to-extracellular radionuclide concentration, (b) the labeled cell density, and (c) the cell size have been examined for the labeled and nonlabeled cells in a cell cluster, and the conditions in which conventional dosimetry underestimates or overestimates the dose to individual cells have been indicated. It is shown that when selective intracellular uptake of a radiolabeled compound occurs in specific cells within a cell cluster, conventional dosimetry underestimates the radiation dose delivered to the labeled cells by twofold to more than 25-fold if the emitted electrons have ranges of a few micrometers or less, i.e., energies smaller than ~10 keV. Under the same conditions, conventional dosimetry overestimates slightly (20% to 50%) the electron radiation dose to the nonlabeled cells of the cell cluster. It is shown that inclusion of photons in the calculation of the total dose to individual cells does not alter significantly the conclusions of the present investigation.

J Nucl Med 30:1856–1864, 1989

The dosimetric methods of the Medical Internal Radiation Dose (MIRD) Committee (*1*) and of the International Commission on Radiation Units and Measurements (ICRU) (*2*) have been invaluable for estimating whole-body and organ doses of radionuclides used in medicine. However, in the determination of radiation hazards, especially with regard to radiation damage to germ and somatic cells of the younger patient and the fetus, the ultimate radiation dose of consequence is not the integrated whole-body or organ dose but the dose to radiosensitive cells in an organ, e.g., stem cells in the bone marrow (*3*). Although in the formulation of the MIRD schema it was recognized that the distribution of uptake and absorbed dose within organs is not uniform, the average absorbed dose was considered to be adequately representative, and in effect the understood assumptions are that the dose to the

individual cell in an organ is the same as the average organ dose (*4*) and that the radionuclide is distributed homogeneously over all cells and the extracellular medium. No distinction is made between agents that concentrate in cells and in the extracellular fluid. Implicit for the validity of this dosimetric approach is that the ranges of ionizing particles emitted are much longer than the average cell diameter (*5*); however, most of the commonly used radionuclides in diagnostic nuclear medicine emit numerous low-energy Auger electrons with subcellular ranges.

During the past several years, in vitro studies have demonstrated that the cell dose is highly dependent on whether or not an Auger electron emitter is internalized by the cells (*6–14*). The importance of selective intracellular localization of the radionuclide has also been reiterated by in vivo experiments in the mouse testes model (*15–17*) in which similar issues have been addressed for thallium-201 (^{201}Tl), indium-111 (^{111}In), iron-55 (^{55}Fe) and iron-59 (^{59}Fe). Although no published studies have demonstrated the concentration of any of these radionuclides in the human testes, signifi-

cant concern with respect to spermatogenesis (3, 18–20) is generated by standard extrapolations of mouse data to man.

As new agents concentrated by cells are employed, other commonly used radionuclides such as ^{123}I and ^{99m}Tc might well appear at high concentrations within the genome of radiosensitive cells (3,21–23). For example, blood cell radiolabeling with ^{111}In and ^{99m}Tc is currently a part of well established diagnostic procedures (24–26), and there has been some concern regarding the radiation dose received by such labeled cells (27), since lymphocytes as well as spermatogonia are known to be quite sensitive to radiation mutagenesis that can lead to oncogenic transformation (28). In view of the individual cell dose estimates and the accompanying risks, the safety of labeling with [^{111}In]oxine to monitor in vivo lymphocyte homing and recirculation has also been questioned (29). Similarly, it has been suggested that labeling lymphocytes with technetium-99m (^{99m}Tc) should be scrutinized carefully and that efforts should be made to reduce the radiation levels to which these cells are exposed (30). Furthermore, it is known that a large fraction of these labeled blood cells concentrate in the liver or spleen a few hours after injection (31). In these cases, the conventional dosimetric assumption that the radionuclide is distributed homogeneously in these organs is probably not true (32). No complete evaluation exists as to what deviations from the actual cell dose might result from this assumption of homogeneous radionuclide deposition.

In an attempt to elucidate some of these questions, we compare a cellular dosimetry approach to the conventional dosimetry approach for various electron energies and for several radionuclides of interest while varying relevant parameters, i.e., intracellular-to-extracellular radionuclide concentration, fraction of organ volume occupied by the labeled cells (corresponding to a particular labeled cell density), and cell size. The results show the extent to which there is reason for concern in nuclear medicine with respect to the dosimetry of intracellular agents and indicate certain situations in which the assumptions of conventional dosimetry break down.

METHODS

Calculations have been carried out to estimate the electron radiation dose to individual cells in a cell cluster (considered the organ) by adopting either conventional or cellular dosimetry approaches. To estimate the radiation dose from electrons received by an individual cell in the cell cluster with the cellular dosimetry approach, the dose contributions from (a) neighboring labeled cells, (b) the extracellular medium, and (c) the cell itself are considered. The radionuclide is assumed to be distributed uniformly throughout the labeled cells; furthermore, each *labeled* cell is assumed to contain the same amount of radioactivity. Because of the absence of electronic equilibrium conditions (33), cells that are located near the surface of the cell cluster will receive a lower dose than cells

well inside the cluster. For large cluster sizes (close to the size of human organs), however, cells that lie just a few cell diameters or more from the cluster surface (i.e., the overwhelming majority of the cells) will be under equilibrium conditions when the emitted electrons are in the keV (or lower) energy region. The present calculations are performed with respect to these cells (target cells).

The first step in the calculation is the choice of a cell cluster geometry. Two geometric models have been reported recently for close-packed cellular structures (7,34,35): the body centered cubic arrangement, assuming each cell to be in contact with eight other cells, and the hexagonal arrangement, assuming each cell to be in contact with 12 other cells. The hexagonal cell arrangement, which seems to represent more realistically the way cells are frequently packed in liquid environments (36), has been adopted in this study. In this geometry, the extracellular space occupies a fraction of 0.26 of the total available space, close to what cytological studies reveal for some human tissues (36). However, the basic conclusions of the present study do not depend strongly on the choice of cluster geometry.

To determine the energy deposited in a target cell from a radioactive decay occurring in another cell that lies at a certain distance in water equivalent medium, analytical calculations are based on the electron energy loss formulae of Cole (37). These formulae are experimental and provide a convenient method to account for the energy loss of both very low and high energy electrons in water equivalent medium. The dose to the target cell is calculated by analytic means (see Appendix I), and a program written in Fortran 77 on a Digital Equipment Corporation VAX 11/780 computer is used to calculate the radiation dose to a target cell of the hexagonal cell cluster arrangement. Briefly, the program operates as follows. The electron range corresponding to a specific electron energy or to the maximum electron energy of the specific radionuclide (37) defines the region from which electrons can reach the cell of interest. The program at first builds spheres in a hexagonal arrangement around the sphere considered (i.e., target sphere) until the further addition of spheres fails to contribute to the electron dose to the target sphere for any particular radionuclide examined (i.e., electronic equilibrium has been achieved for the target sphere). The radii of these arbitrarily chosen spheres are equal to or larger than the radii of the cells. Next, the distance from the center of each sphere to the target sphere is calculated. The cells are assumed to be spheres of a chosen diameter, situated concentrically to the ones already constructed. The sphere placed concentrically to the target sphere represents the target cell. Variation of the radii of the two concentric sets of spheres provides the dependence of the present model on cell size and the fraction of organ volume occupied by the cells (f). Thus, if the radius of the first set of spheres is equal to the radius of the second set of spheres (cells), a closed-packed cell arrangement is simulated and the cells occupy a fraction f = 0.74 of the total cluster volume. If the radius of the first set of spheres is increased relative to the radius of the cells, the cell-to-cell distances also increase and the cells occupy smaller fractions of the overall cluster volume. As an example, when the labeled cells are at distances of 25 and 50 μm from each other (center-to-center), the corresponding values of f are 0.015 and 0.0015. The computer program then sums up the electron dose con-

tributions to the target cell from all surrounding cells and adds to that the radiation dose component from the extracellular medium for a given radionuclide concentration. The latter dose component is calculated by determining the dose that would be delivered to the target cell from an arbitrary concentration of uniformly distributed radionuclide over the whole space and subtracting the dose from surrounding cells for the same radionuclide concentration. Thus, different intracellular-to-extracellular radioactivity concentrations (k) are taken into consideration. Finally, the radiation dose of the target cell to itself is calculated according to the methods described by Kassis et al. (9).

For the conventional calculation of electron dose, no distinction is made between spheres and medium and the radionuclide is assumed to distribute homogeneously throughout the volume considered. In the present model, this is equivalent to having the same concentration of radionuclide inside all the cells within the cluster as well as throughout the extracellular space (f = 0.74, k = 1). Thus, the dose to the target cell

is the same as the overall organ dose or any other subvolume chosen. In this paper, the average radioactivity concentration within the whole cell cluster has always been normalized to a standard radioactivity concentration (it makes no difference what concentration is chosen, as the results are presented as a ratio of the two dosimetry models). As a direct check of the computations performed, we compared our cellular dosimetry approach for the pure beta emitter ^{90}Y (using k = 1 and f = 0.74) to the one published by MIRD for large human organs, e.g., liver (38–41); the two agree to within 5%. This small difference in the absolute dose value is assumed to originate in the different methods for dose derivation used in the two treatments. Since the energy-loss formulae of Cole (37) were used in both the cellular and the conventional dose calculations in this work and the results are presented as the ratio of cellular-to-conventional dosimetry estimates, the difference in using either the formulae of Cole or the dose point kernels of Berger (38) are, therefore, expected to be very small.

The radionuclides studied were ^{99m}Tc, ^{201}Tl, ^{123}I, and ^{111}In,

TABLE 1
Average Emission Spectra for the Isotopes Examined in the Present Calculations*

^{99m}Tc		^{201}Tl		^{111}In		^{123}I	
Yield/ decay	Energy (keV)	Yield/ decay	Energy (keV)	Yield/ decay	Energy (keV)	Yield/ decay	Energy (keV)
Electrons							
0.023	16.3	0.034	61.07	0.144	20.1	0.128	24.3
0.114	2.11	0.79	8.47	1.03	2.69	0.976	3.27
0.062	0.368	2.12	1.874	2.08	0.351	0.134	0.670
1.0	0.220	0.056	1.388	0.149	0.182	1.9	0.475
0.28	0.144	0.22	0.709	0.925	0.124	0.065	0.258
0.48	0.110	0.50	0.427	2.54	0.039	0.167	0.210
0.038	0.067	0.90	0.260	1.13	0.012	0.190	0.154
2.03	0.035	2.80	0.157	0.085	144.6	0.472	0.110
0.984	1.77	6.86	0.090	0.013	168.1	2.5	0.065
0.119	122.0	0.46	0.062	0.050	218.6	0.18	0.048
		2.96	0.038	0.009	241.9	3.52	0.027
		2.05	0.025			0.75	0.015
		0.334	0.786			0.136	127.2
		0.034	1.454			0.018	154.1
		0.0015	12.24			0.004	158.0
		0.0005	24.02				
		0.082	15.84				
		0.025	27.74				
		0.07	17.43				
		0.022	29.34				
		0.0075	52.24				
		0.017	123.4				
		0.158	84.3				
		0.034	155.3				
Photons							
0.889	140.5	0.100	167.4	0.905	171.3	0.828	0.159
		0.462	70.8	0.940	245.4		
		0.272	68.9	0.443	23.2		
		0.105	80.2	0.236	23.0		
		0.19	9.98				
		0.182	11.85				

* Only major emissions are listed. The low-energy electron spectra have been taken from Sastry et al. (4) and Rao et al. (15).

all of which are currently employed in nuclear medicine procedures. The detailed Auger and conversion electron spectra emitted by these radionuclides were taken from Sastry et al. (4) and from Rao et al. (15). Table 1 is a concise compilation of the principal emissions of these radionuclides.

The contribution of photons emitted by the radionuclides to the total radiation dose of the target cell can be accounted for by adding the MIRD estimate of the dose contributed by photons to both the cellular and the conventional calculation; this can be done because photons have a long range of action and, in this case, the assumption of a homogeneous radionuclide distribution throughout the cell cluster is adequately valid. The photon dose estimates for various human organs (i.e., different cluster sizes) have been obtained from the published conventional dosimetry tables (39–41). The photon dose contribution to the total radiation dose increases with increasing cell cluster size and consequently the overall cellular-to-conventional dose ratio is closer to unity as the cell cluster size increases. The total radiation dose to the target cell from both photons and electrons emitted by ^{99m}Tc is presented in the RESULTS AND DISCUSSION section for cell cluster sizes corresponding to specific human organs.

FIGURE 1
Ratio of cellular-to-conventional dosimetry estimates for individual cell (d = 10.3 μm) in cell cluster as function of emitted electron energy, for three values of cluster volume fraction (f = 0.74, 0.13, 0.01) occupied by labeled cells and for intracellular-to-extracellular radionuclide concentration (k) 100. Also shown is the case for f = any and k = 1.

RESULTS AND DISCUSSION

The results of the present dosimetric investigation are presented in Figures 1 through 4. Electrons only are considered in these figures, although a comment on the effect of the inclusion of photons has also been included.

Figure 1 shows the ratio of the cellular to conventional dosimetric estimates as a function of the emitted electron energy for three different values of the cell cluster volume fraction occupied by the labeled cells (f) and for two values of the intracellular-to-extracellular radionuclide concentration (k). The cell diameter in Figure 1 was chosen to be 10.3 μm (V79 Chinese hamster lung fibroblasts). It can be seen that for close-packed labeled cells (f = 0.74), the cellular and the conventional dosimetric estimates do not differ significantly if (a) the cells are closely packed (f ~ 0.74) or (b) the intra- and the extracellular concentrations are the same (k ~ 1). Also, if the radionuclide remains primarily in the extracellular space (k ≪ 1), then the cellular and the conventional dosimetry estimates are similar, except for very low electron energies where small differences occur (data not shown). However, when the radionuclide is concentrated selectively by certain cells (k ≫ 1 and f ≪ 0.74), the cellular-to-conventional dosimetry estimates deviate significantly from unity for the low energy electrons with ranges comparable to or smaller than the cell diameter (E < 10 keV), and conventional dosimetry seriously underestimates the delivered dose at the cellular level.

Figure 2 depicts the ratio of cellular to conventional dosimetric estimates for the electrons emitted by each of the four radioisotopes as a function of the cell cluster volume occupied by the labeled cells (f), for four intra-
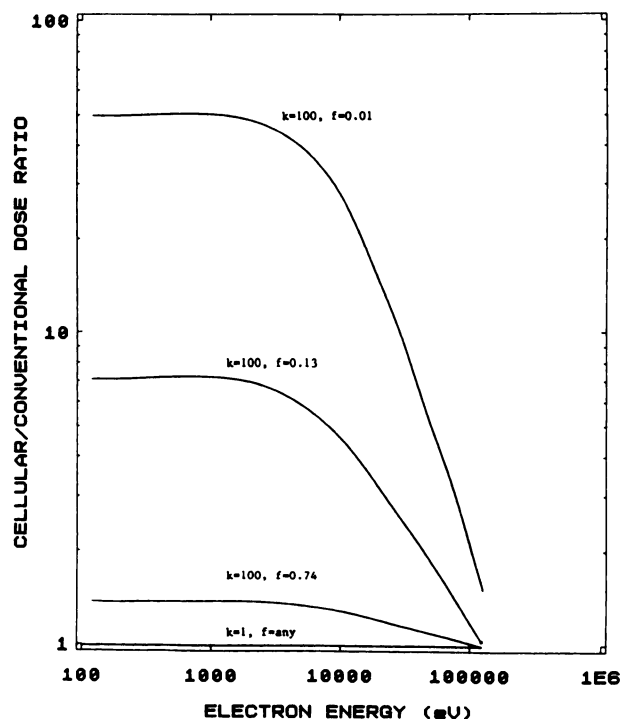
cellular-to-extracellular radionuclide concentrations (k = 1000, 100, 1, 0.01). A cell diameter of 10.3 μm was also chosen for these calculations. The results indicate that when f < 0.2 and k ≫ 1, the ratio of the cellular to conventional dosimetric estimates deviates by factors of 2 to 25 from unity. In fact, as f decreases further, the ratio increases even more. This deviation is determined to a large extent by the number and the energies of the higher energy electrons (energetic conversion electrons or beta particles) emitted per decay. For example, although ^{123}I emits on the average a larger number of short range Auger electrons than ^{111}In (11 versus 8 electrons on average, respectively, (4, 15)), the cellular to conventional dosimetry ratio rises more steeply for the latter radionuclide because the abundance of the energetic conversion electrons emitted by ^{123}I is greater than that of ^{111}In while the electron energies are similar.

Finally, when the radionuclide is excluded from the cells (k ≪ 1), conventional dosimetry overestimates the electron dose delivered to the labeled cells by ~20% (curve 4).

The deviation of the cellular-to-conventional dose ratio from unity in Figure 2 for f < 0.2 and k ≫ 1 is

FIGURE 2
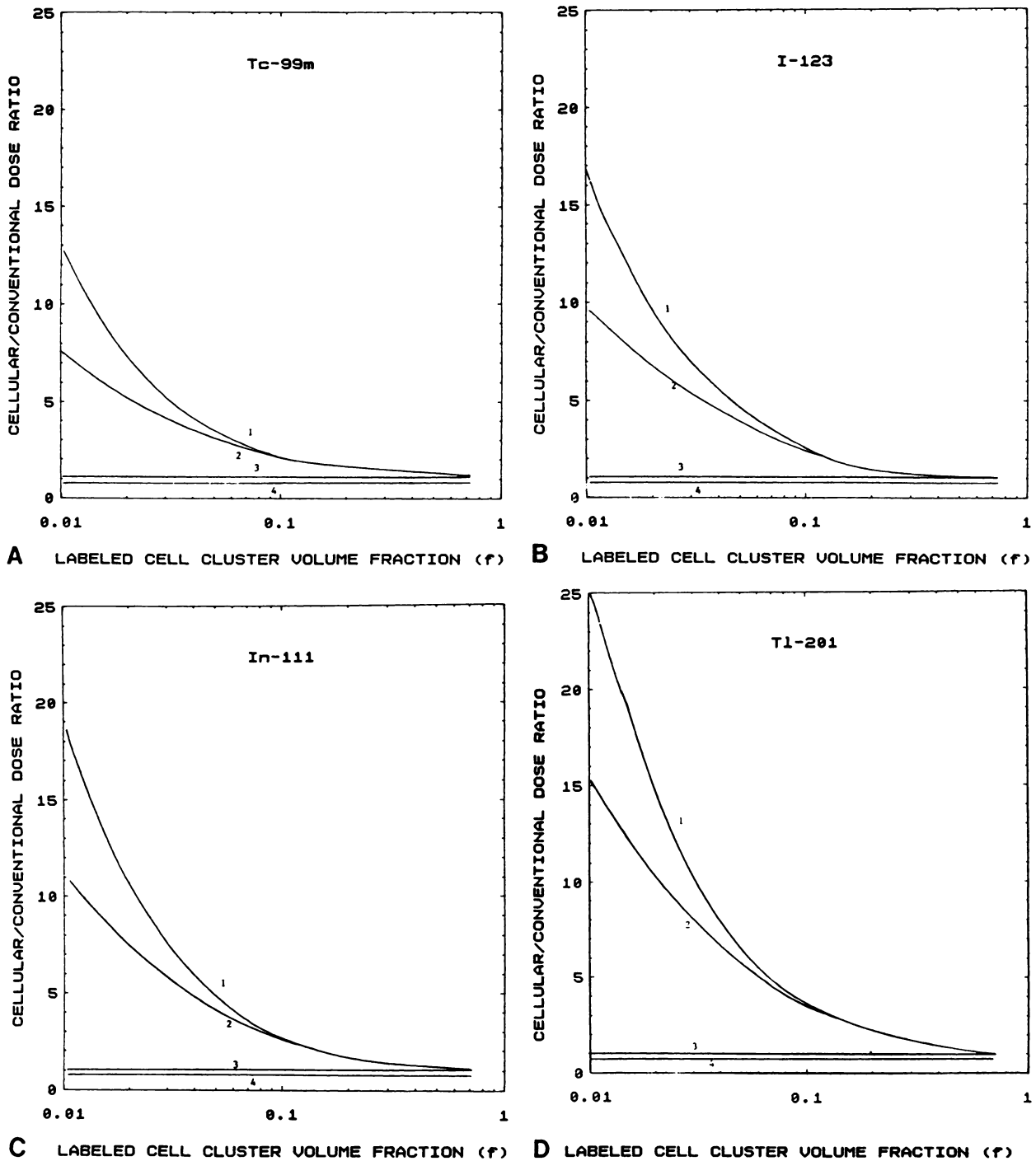
Ratio of cellular-to-conventional dosimetry estimates for individual cell (d = 10.3 μm) in cell cluster for (a) ^{99m}Tc, (b) [123]I, (c) [111]In and (d) ^{201}Tl as function of cell cluster volume occupied by labeled cells (f) for various intracellular-to-extracellular radionuclide concentrations (k). Curve 1: k = 1000. Curve 2: k = 100. Curve 3: k = 1. Curve 4: k = 0.01. Electrons only are considered in this figure. For an estimate of the influence of the emitted photons, see text.

somewhat lessened if the photon dose delivered by the radionuclides is accounted for. The degree to which this occurs depends on the size of the cellular cluster considered. For example, for ^{99m}Tc and cellular cluster sizes corresponding to the size of human ovaries, testes, spleen, and liver, the cellular-to-conventional dose ratio

for k = 100 and f = 0.01 has values of 6.6, 6.1, 5.4, and 4.0, respectively, when both photons and electrons are included in the calculation; however, the general shape of the curves in Figure 2 remains the same. For electrons only, a single value of 7.4 is obtained; therefore, the results are not substantially different from those ac-
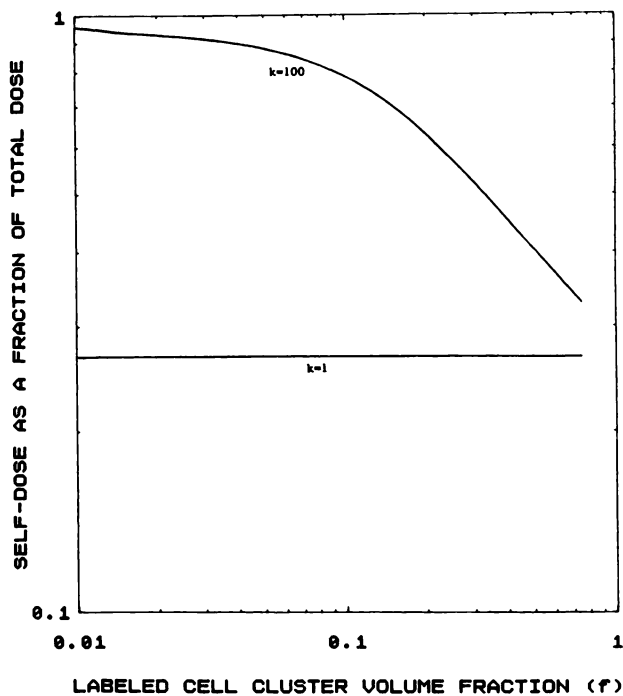
Tl-201

LABELED CELL CLUSTER VOLUME FRACTION (f)

FIGURE 3
Fraction of total radiation dose delivered by electrons to ^{201}Tl-labeled cell (d = 10.3 μm) in cell cluster due to decays within cell (self-dose) for two intracellular-to-extracellular radionuclide concentrations (k) and various cluster volume fractions occupied by labeled cells (f).

counting only for the electrons, and the presence of photons does not change the basic conclusions derived from the present results.

The fraction of the total radiation dose emanating from intracellular decays and deposited within the cell itself (self-dose), as derived with the cellular dosimetry model, is depicted in Figure 3 for ^{201}Tl. The results indicate that for high intracellular concentration (k $\gg$ 1) and low values of f, most of the radiation dose delivered is due to self-irradiation. Thus, the increase in the cellular-to-conventional dosimetric ratio in Figure 2 for k $\gg$ 1 and f < 0.2 is mostly due to the increasing contribution of the self-dose when the radioactivity moves from the extracellular regions into the cell. Similar conclusions have been reached for the other three Auger electron emitters.

Figure 4 shows the influence of cell size on the dose from ^{123}I received by an individual cell in a cell cluster. When the radionuclide concentrates selectively (f < 0.2) and highly (k $\gg$ 1) in certain cells, there is a gradual increase of the cellular dose with increasing cell diameter and consequently the ratio of the cellular to conventional dose increases too. Here again, similar results are obtained with the other three radionuclides.

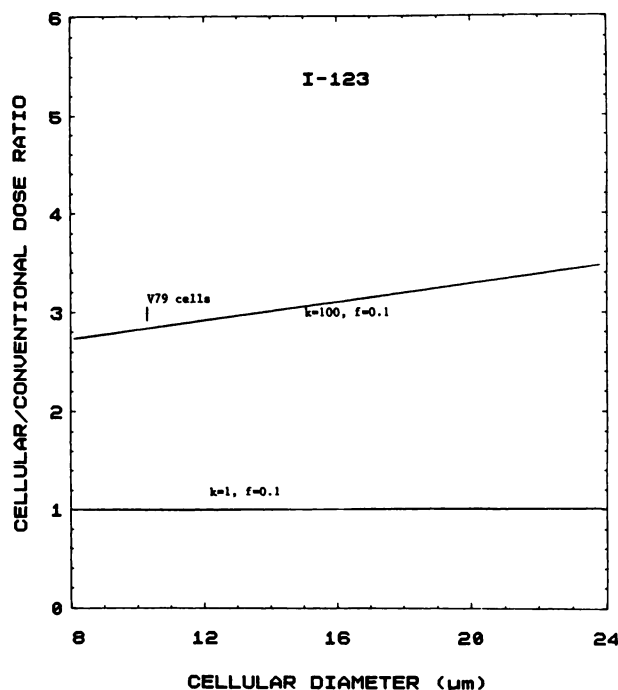Finally, the ratio of the cellular to conventional dose

FIGURE 4
Ratio of cellular-to-conventional dosimetry estimates for labeled cell in cell cluster for ^{123}I, as function of cell diameter for two values of intracellular-to-extracellular radionuclide concentration (k) and for f = 0.1. Electrons only are considered in this figure.

was calculated for the nonlabeled cells of a cell cluster where radionuclide uptake occurs only in specific cells. The results for ^{99m}Tc, ^{201}Tl, ^{123}I, and ^{111}In show that the electron radiation dose to the nonlabeled cells of the cluster, originating from decays in the extracellular medium and in the labeled cells, is generally 20 to 30% smaller than that predicted by conventional dosimetry. At high values of the intracellular-to-extracellular concentration ratio (k > 100) and very small values of labeled cell cluster volume fraction (f $\ll$ 0.74), some nonlabeled cells in the cluster receive practically zero dose from electrons because of the short ranges of the latter. In practice, these cells receive only photon dose contributions.

In view of the fact that (a) most of the radionuclides used in diagnostic nuclear medicine, including those examined, emit several low-energy electrons and (b) situations of selective radionuclide concentration by specific cells in an organ are common, the present calculations seem to be of some importance. A typical example is the case of ^{99m}Tc-labeled albumin colloid (Microlite) that is routinely used in the clinic for liver imaging. These colloidal particles would be expected to be selectively taken up by liver macrophages (Kupffer cells) since these cells are known to fix and phagocytose circulating foreign material (42). In fact, these particles have been shown to be avidly phagocytosed by rat liver Kupffer cells (43, 44). Recently, a quantitative study

on the selective concentration of injected radiolabeled Microlite in mouse liver Kupffer cells has been performed using autoradiography and quantitative video-densitometric methods (Makrigiorgos GM, Bara-nowska-Kortylewicz J, Vinter DW, et al: unpublished data). As macrophages are randomly situated throughout the organ, the labeled cell geometry resembles the one assumed in the present model. Thus, it was shown that conventional dosimetry underestimates by factors of 8 to 30 (corresponding to k = 200–1000 and f = 0.001–0.01) the radiation dose delivered by ^{99m}Tc-labeled colloids to the macrophages of the liver (photons were included in the dosimetry). Similar conclusions are valid for the macrophages of the spleen, lung, and bone marrow.

The possible biologic consequences of such dosimetric inaccuracies clearly depend on the radiosensitivity of the labeled cells. In general, little is known about the radiosensitivity of particular cell lines in most human organs. With the continual generation of new diagnostic radiopharmaceuticals suitable for imaging, elucidation of such considerations becomes increasingly important. Radiobiologic studies (in vitro and in vivo) as well as dosimetric analysis at the cellular level may provide useful information regarding these issues.

APPENDIX 1

Determination of the Average Energy Deposited in Sphere O Per Decay in Sphere O' for Electrons

The formula given by Cole (30) for the electron energy loss dE/dR (eV/nm) by an electron with energy E (eV) and residual range R (nm) in water equivalent medium is:

$$dE/dR = 67.3 \cdot (R + 7)^{-0.435} + 5.63 \cdot 10^{-4} \cdot R^{0.33},$$

where R is related to the electron energy by:

$$E(R) = 119.1 \cdot (R + 7)^{0.565} + 4.23 \cdot 10^{-4} \cdot R^{1.33} - 367.$$

At a distance r from the decay site, the electron has a residual range of

$$R = R_{tot} - r,$$

where R_{tot} is the electron range corresponding to the initial energy of the electron, immediately following its ejection by the radionuclide. Consequently the energy absorbed dE in the annular region of a spherical shell with radii r and r + dr centered around the site of decay is given by (9):

$$dE = dr \cdot dE/dR \Big|_{R_{tot}-r} \quad 0 < r < R_{tot}.$$

These formulae are valid over the electron energy region from 20 eV to 20 MeV.

Consider the geometry of Figure A1. The two equal size spheres of radius R_N represent cells at a distance u (center-to-center) from each other. The average energy dE_A deposited in sphere O per decay occurring at a random point A within sphere O' is given by:

$$dE_A = \int_{p-R_N}^{p+R_N} 0.5 \cdot (1 - \cos \theta) \cdot dE/dr \cdot dr,$$

where p is the distance from A to O and $\cos \theta = (r^2 + p^2 - R_N^2)/2rp$. The segment of the spherical shell with radius (p) centered at O which intersects sphere O' is equal to $(2\pi p) \cdot p \cdot (1 - \cos \phi)$, where $\cos \phi = (u^2 + p^2 - R_N^2)/2up$. Hence, the total energy deposited in sphere O per decay in sphere O' is given by:

$$E_{OO'} = \int_{u-R_N}^{u+R_N} 2\pi p^2 (1 - \cos \theta)/(4\pi R_N s/3)$$

$$\cdot \int_{p-R_N}^{p+R_N} 0.5 \cdot (1 - \cos \theta) dE/dr \cdot dr dp,$$

where the factor $4\pi R_N^3/3$ was introduced to convert on a 'per decay' basis.

Finally, when a number of electrons having different energies are emitted by the radionuclide, the energy deposited in O' is calculated by summing the contributions from each electron.
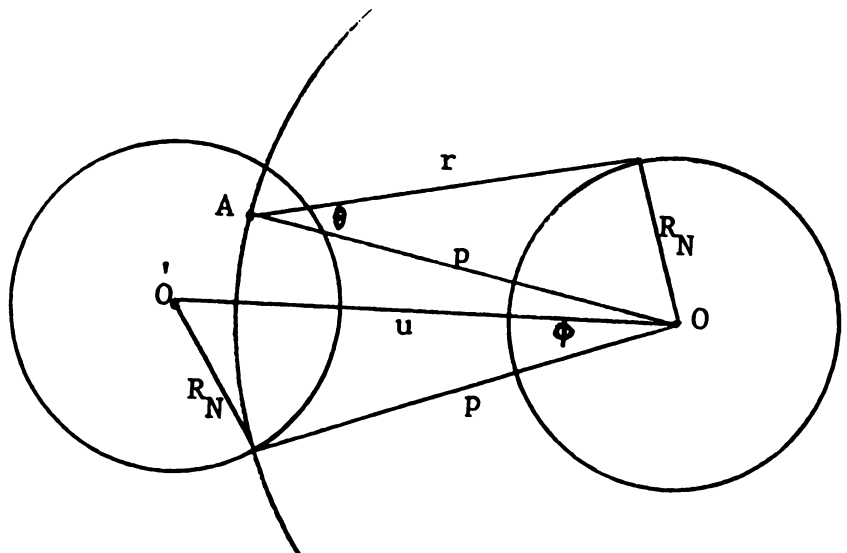

FIGURE A1
Geometry assumed for estimation of energy deposited by electrons in one cell per decay of uniformly distributed isotope in another cell.

ACKNOWLEDGMENT

REFERENCES

1. Loevinger R, Berman M. A revised schema for calculating the absorbed dose from biologically distributed radionuclides. *MIRD Pamphlet No 1, Revised.* New York: The Society of Nuclear Medicine, 1976.

2. ICRU Report 32: Methods of assessment of absorbed dose in clinical use of radionuclides. Washington, DC: International Commission on Radiation Units and Measurements, 1979.

3. Gaulden ME. "Biological dosimetry" of radionuclides and radiation hazards. *J Nucl Med* 1983; 24:160–164.

4. Sastry KSR, Rao DV. Dosimetry of low energy electrons. In: Rao DV, Chandra R, Graham MC, eds. *Physics of nuclear medicine: recent advances.* American Association of Physicists in Medicine Monograph No 10. New York: American Institute of Physics, 1984: 169–208.

5. Adelstein SJ, Kassis AI, Sastry KSR. Cellular vs. organ approaches to dose estimates. In: *Proceedings of the Fourth International Radiopharmaceutical Dosimetry Symposium.* Oak Ridge, TN: CONF-851113 (DE86010102), 1985: 477–492.

6. Kassis AI, Adelstein SJ, Haydock C, Sastry KSR, McElvany KD, Welch MJ. Lethality of Auger electrons from the decay of bromine-77 in the DNA of mammalian cells. *Radiat Res* 1982; 90:362–373.

7. Kassis AI, Adelstein SJ, Haydock C, Sastry KSR. Thallium-201: an experimental and a theoretical radiobiological approach to dosimetry. *J Nucl Med* 1983; 24:1164–1175.

8. Kassis AI, Sastry KSR, Adelstein SJ. Intracellular distribution and radiotoxicity of chromium-51 in mammalian cells: Auger-electron dosimetry. *J Nucl Med* 1985; 26:59–67.

9. Kassis AI, Adelstein SJ, Haydock C, Sastry KSR. Radiotoxicity of ^{75}Se and ^{35}S: theory and application to a cellular model. *Radiat Res* 1980; 84:407–425.

10. Chan PC, Lisco E, Lisco H, Adelstein SJ. The radiotoxicity of iodine-125 in mammalian cells. II. A comparative study on cell survival and cytogenetic responses to ^{125}IUdR, ^{131}IUdR, ^{3}HTdR. *Radiat Res* 1976; 67:332–343.

11. Hofer KG, Hughes WL. Radiotoxicity of intracellular tritium, ^{125}iodine and ^{131}iodine. *Radiat Res* 1971; 47:94–109.

12. Burki HJ, Rotts R, Feinendegen LE, Bond VP. Inactivation of mammalian cells after disintegrations of ^{3}H or ^{125}I in cell DNA at −196°C. *Int J Radiat Biol* 1973; 24:363–375.

13. Bradley EW, Chan PC, Adelstein SJ. The radiotoxicity of iodine-125 in mammalian cells. I. Effects on the survival curve of radioiodine incorporated into DNA. *Radiat Res* 1975; 64:555–563.

14. Hofer KG, Harris CR, Smith JM. Radiotoxicity of intracellular ^{67}Ga ^{125}I and ^{3}H. Nuclear versus cytoplasmic radiation effects in murine L1210 leukemia. *Int J Radiat Biol* 1975; 28:225–241.

15. Rao DV, Sastry KSR, Grimmond HE, et al. Cytotoxicity of some indium radiopharmaceuticals in mouse testes. *J Nucl Med* 1988; 29:375–384.

16. Rao DV, Govelitz GF, Sastry KSR. Radiotoxicity of thallium-201 in mouse testes: inadequacy of conventional dosimetry. *J Nucl Med* 1983; 24:145–153.

17. Rao DV, Sastry KSR, Govelitz GF, Grimmond HE, Hill HZ. In vivo effects of iron-55 and iron-59 on mouse testes: biophysical dosimetry of Auger electrons. *J Nucl Med* 1985; 26:1456–1465.

18. Heller CG, Wotton P, Rowley MJ, et al. Action of radiation upon human spermatogenesis. *Excerpta Med Intern Congr Ser* 1965; 112:408–410.

19. Oakberg EF. Duration of spermatogenesis in the mouse and timing of stages of the cycle of the seminiferous epithelium. *Am J Anat* 1956; 99:507–516.

20. Vidal F, Templado C, Navardo J, et al. Meiotic and synaptonemal complex studies in 45 subfertile males. *Human Gen* 1982; 60:301–304.

21. Winchell HS, Baldwin RM, Lin TH. Development of I-123-labeled amines for brain studies: localization of I-123 iodophenylalkyl amines in rat brain. *J Nucl Med* 1980; 21:940–946.

22. Piwnica-Worms D, Kronauge JF, Holman BL, Lister-James J, Davison A, Jones AG. Hexakis (carbomethoxyisopropylisonitrile)technetium (I), a new myocardial perfusion imaging agent: binding characteristics in cultured chick heart cells. *J Nucl Med* 1988; 29:55–61.

23. Froelich J. Nuclear medicine in inflammatory diseases. In: Freeman LM, Weissmann HS, eds. *Nuclear medicine annual 1985.* New York: Raven Press, 1985: 23–70.

24. McAfee JG, Gagne GM, Subramanian G, et al. Distribution of leukocytes labeled with In-111 oxine in dogs with acute inflammatory lesions. *J Nucl Med* 1980; 21:1059–1068.

25. Goedemans WTH. Simplified cell labeling with In-111 acetylacetone [Abstract]. *Br J Radiol* 1981; 54:636–637.

26. Dewanjee MK, Rao SH. Red cell membrane permeability and metal oxine-hemoglobin transchelation: implication in cell labeling [Abstract]. *J Labelled Compd Radiopharm* 1981; 18:280–281.

27. Segal AW, Deteix P, Garcia R, Tooth P, Zanelli GD, Allison AC. Indium-111 labeling of leukocytes: a detrimental effect on neutrophil and lymphocyte function and an improved method of cell labeling. *J Nucl Med* 1978; 19:1238–1244.

28. Cronkite EP, Bond VP. *Radiation injury in man.* Springfield, IL: CC Thomas Publisher, 1960.

29. Chisholm PM, Danpure HJ, Healey G, Osman S. Cell damage resulting from the labeling of rat lymphocytes and HeLa S3 cells with In-111 oxine. *J Nucl Med* 1979; 20:1308–1311.

30. Parmentier C, Chavaudra J, Meignan M. Dose received by lymphocytes in the course of labeling techniques using Tc-99m [Letter]. *J Nucl Med* 1978; 19:223.

31. Goodwin DA, Finston RA, Smith SI. The distribution and dosimetry of In-111 labeled leukocytes and platelets in humans. In: *Third International Radiopharmaceutical Dosimetry Symposium.* HHS publication FDA 81-8166; 1981: 88–101.

32. Watson EE. Cell labeling: radiation dose and effects. *J Nucl Med* 1983; 24:637–640.

33. Loevinger R. Discrete radioisotope sources. In: Hine GJ, Brownell GL, eds. *Radiation dosimetry.* New York: Academic Press; 1956: 716–776.

34. Bigler RE, Cosma M, Zanzonico PB, Sgouros G. Electron and α-particle radioimmunotherapy dosim-

etry for micrometastases. In: *Symposium on Radiation Carcinogenesis and Dosimetry*, Memorial Sloan Kettering Center, New York, April 28, 1986: 42–68.

35. Sastry KSR, Haydock C, Basha AM, Rao DV. Electron dosimetry for radioimmunotherapy: optimal electron energy. *Radiat Prot Dos* 1985; 13:249–252.

36. Thomson DW. *On growth and form*. Cambridge: The University Press; 1963: 465–553.

37. Cole A. Absorption of 20 eV to 50,000 eV electron beams in air and plastic. *Radiat Res* 1969; 38:7–33.

38. Berger MJ. Beta-ray dosimetry calculations with the use of point kernels. In: Cloutier RJ, Edwards CL, Snyder WS, eds. *Medical radionuclides: radiation dose and effects*. USAEC Report CONF-691212; 1970:63–86.

39. Brownell GL, Ellett WH, Reddy AR. Absorbed fractions for photon dosimetry. MIRD Pamphlet No 3. *J Nucl Med* 1968; 9(suppl 1):27–39.

40. Snyder WS, Ford MR, Warner GG, Fisher HL Jr.

Estimates of absorbed fractions for monoenergetic photon sources uniformly distributed in various organs of a heterogeneous phantom. MIRD Pamphlet No 5, *J Nucl Med* 1969; 10(suppl 3):5–52.

41. Snyder WS, Ford MR, Warner GG, Watson SB. "S", absorbed dose per unit cumulated activity for selected radionuclides and organs. *MIRD Pamphlet No 11*. New York: The Society of Nuclear Medicine; 1975.

42. Wisse E, Knook DL. The investigation of sinusoidal cells: a new approach to the study of liver function. In: Popper H, Schaffner F, eds. *Progressive liver diseases*, Vol 6. New York: Academic Press; 1979: 153–167.

43. Hindie E, Colas-Linhart N, Petiet A, Bok B. Microautoradiographic study of technetium-99m colloid uptake by the rat liver. *J Nucl Med* 1988; 29:1118–1121.

44. Sands H, Jones PL. Methods for the study of the metabolism of radiolabeled monoclonal antibodies by liver and tumor. *J Nucl Med* 1987; 28:390–398.